



HAL
open science

Structure and dynamics of ice Ih films upon HCl adsorption between 190 and 270 K. II. Molecular dynamics simulations

Céline Toubin, Sylvain Picaud, Paul N.M. N M Hoang, Claude Girardet, Benjamin Demirdjian, Daniel Ferry, Jean Suzanne

► **To cite this version:**

Céline Toubin, Sylvain Picaud, Paul N.M. N M Hoang, Claude Girardet, Benjamin Demirdjian, et al.. Structure and dynamics of ice Ih films upon HCl adsorption between 190 and 270 K. II. Molecular dynamics simulations. *The Journal of Chemical Physics*, 2002, 116 (12), pp.5150. 10.1063/1.1454991 . hal-03003068

HAL Id: hal-03003068

<https://hal.science/hal-03003068>

Submitted on 19 May 2021

HAL is a multi-disciplinary open access archive for the deposit and dissemination of scientific research documents, whether they are published or not. The documents may come from teaching and research institutions in France or abroad, or from public or private research centers.

L'archive ouverte pluridisciplinaire **HAL**, est destinée au dépôt et à la diffusion de documents scientifiques de niveau recherche, publiés ou non, émanant des établissements d'enseignement et de recherche français ou étrangers, des laboratoires publics ou privés.

Structure and dynamics of ice Ih films upon HCl adsorption between 190 and 270 K. II. Molecular dynamics simulations

C. Toubin, S. Picaud, P. N. M. Hoang, C. Girardet^{a)}

Laboratoire de Physique Moléculaire—UMR CNRS 6624, Faculté des Sciences, La Bouloie, Université de Franche-Comté, F-25030 Besançon Cedex, France

B. Demirdjian, D. Ferry, and J. Suzanne

CRMC2-CNRS,^{b)} Campus de Luminy, Case 913, F-13288 Marseille Cedex 9, France

(Received 27 June 2001; accepted 7 January 2002)

Classical molecular dynamics simulations are carried out between 190 and 250 K on an ultrathin ice film doped by HCl deposition with a coverage varying from 0.3 to 1.0 monolayer. These conditions are similar to those defined in the experiments described in the companion paper. Within the assumption that the hydracid molecule remains in its molecular form, the order parameters and the diffusion coefficients for the H₂O molecules are determined in the HCl doped ice film, and compared to the experimental data. The residence times of HCl at the ice surface are also calculated. Below 200 K, the HCl molecules are found to remain localized at the ice surface, while above 200 K, the HCl diffusion inside the film is easy and leads to a strong disorder of the ice structure. Although the formation of hydrates cannot be interpreted by the present calculations, the lowering of the ice melting temperature by 15 K measured in neutron experiments for an HCl doped ice film is qualitatively explained by simulation results. © 2002 American Institute of Physics.

[DOI: 10.1063/1.1454991]

I. INTRODUCTION

The adsorption of HCl on ice has been among the most widely studied process connected to stratospheric science, due to its large influence on the chlorine production responsible for ozone depletion.^{1–3} From a theoretical point of view, one of the most challenging problem was to determine whether the adsorbed hydracid could diffuse in its molecular form inside bulk ice or remained at the ice surface, before being ionized and ultimately dissociated.^{4–12}

Many studies were devoted to the calculation of the adsorption energy, equilibrium configuration and surface residence times of HCl on ice using molecular dynamics (MD) simulations.^{4,6} The results indicated the formation of a strong H-bond between HCl and a water molecule, for which the hydracid acts as a proton donor without dissociating. Gertner and Hynes^{5,7} proposed a model in which the HCl molecules were encapsulated by the evaporated and redeposited water molecules at the surface of ice above 190 K. These authors used *ab initio* simulations to show that the HCl ionization on ice at 190 K was thermodynamically favorable and kinetically rapid at the ice interface. From the MD analysis of the enhanced rotational mobility of the water molecules at the ice surface above 190 K, Kroes¹¹ concluded that this mobility could be responsible for the very efficient adsorption of HCl on ice by allowing the hydracid molecule to dissociate into ions at the ice surface. The resulting interaction between the Cl[−] ion and the surface could explain the high surface coverages observed experimentally. *Ab initio* studies per-

formed at 0 K on small aggregates HCl-(H₂O)_n ($n=1,2,3$, and 4) showed that a critical size of the aggregate ($n=4$) was required to dissociate the HCl molecule by proton transfer through the H-bond network of the H₂O molecules.^{9,10} Svanberg *et al.*⁸ also studied the sticking of HCl on the basal plane of ice at 100, 150, and 200 K, using mixed (QM/MM) molecular dynamics simulations. They showed that HCl ionization could be very efficient at the ice surface depending on the binding process. The mechanism was stated as follows: if the Cl atom of the hydracid was bound to one water dangling hydrogen, HCl adsorbed molecularly, while if two dangling hydrogens were available at the ice surface, HCl could dissociate to the Cl-H₃O⁺ contact ion pair.

Although the approaches of Hynes *et al.*^{5,7} and Svanberg *et al.*⁸ led ultimately to HCl dissociation, the mechanisms by which this dissociation could occur were conceptually different. They opened the question about the times which were allowed for HCl surface adsorption, ice penetration, ionization and finally dissociation, depending on the structure and dynamics of the condensed medium. Classical MD simulations were carried out to analyze the passage of the hydracid molecule from the adsorbed state towards the embedded state inside bulk ice.¹³ The results indicated that the HCl molecule was trapped at the ice interface at 200 K, for a relatively long time (~ 100 ps). No further diffusion of the hydracid was allowed into the bulk. However, at the interface, HCl adopted favorable configurations for proton transfer with its neighboring water molecules over a time scale of about 3–5 ps.

All the previous calculations^{4–11} were performed by considering a single HCl molecule, thus disregarding the influence of collective processes. In fact, when HCl molecules are

^{a)} Author to whom correspondence should be addressed. Electronic mail: claude.girardet@univ-fcomte.fr

^{b)} Also associated with the Universities of Aix-Marseille II and III.

adsorbed on ice from submonolayer up to monolayer coverage, the water structure and dynamics should be dramatically modified. In the companion paper [paper I (Ref. 14)], an experimental study based on quasielastic neutron scattering (QENS) of HCl layers adsorbed on an ultrathin ice film deposited on MgO(001) was made to understand this collective influence. In the present paper, classical MD simulations are carried out to analyze the motions of HCl molecules adsorbed on a water film supported on MgO(001) in the temperature range 190–250 K. The simulations reproduce conditions similar to those realized in the QENS study. The translational and orientational order parameters and the corresponding diffusion coefficients related to the dynamics of the HCl and ice layers are first calculated using semiempirical potentials. Then, the translational and orientational mobilities of the water molecules in the film are compared to those determined from the evolution of the quasielastic profile shape with temperature (paper I).

Let us mention that one advantage of classical MD rests on the possibility to consider finite coverages, as in the experiments, although such calculations made the assumption that the HCl molecules are not ionized in ice. In fact, there is general agreement that hydracids like HCl and HBr might be ionized above 190 K. Such a feature should lead to severe limitations in the validity of the present approach based on molecular diffusion. Nevertheless, there is outstanding issues in the literature about exactly *when* and *where* the molecules are ionized. Therefore, it appears interesting to discuss the consequences of the presence of molecular HCl on the structure and dynamics of doped ice, i.e., without considering any ionization process. This would allow us to distinguish in the experimental data the signatures of the molecular and ionized forms of the hydracid molecule.

In Sec. II, the details of the MD simulations are given, and the results on the order parameters and diffusion coefficients are presented. The comparison between experimental measurements and calculated structural and dynamical properties of the ice film is done in Sec. III. In addition, these results are also compared to MD simulations performed on pure ice,¹⁵ and to those carried out for a single HCl molecule in ice.¹³

II. MOLECULAR DYNAMICS SIMULATION

A. Theoretical backgrounds

1. Interaction potential

The system formed by the MgO substrate, the water molecules and the HCl molecules requires to define a set of five interaction potentials, as

$$V = V_{ws} + V_{ps} + V_{ww} + V_{pp} + V_{wp}, \quad (1)$$

where V_{ws} and V_{ps} are the water/MgO substrate and HCl/MgO substrate potentials, respectively, while the three other potentials V_{ww} , V_{pp} , and V_{wp} characterize the H₂O–H₂O, HCl–HCl, and H₂O–HCl interactions.

The interaction potentials V_{ws} and V_{ps} between the H₂O or HCl molecules and the MgO substrate have been already detailed elsewhere.^{15–17} They are expressed as the sum of a dispersion-repulsion contribution represented by pairwise

atom–atom Lennard-Jones interactions and of electrostatic terms. These latter terms describe the interaction between the electric field and field gradient created by the ionic substrate charges and the point dipoles and quadrupoles of the HCl and water molecules.^{17,18} The polarization effects between the adsorbate and the substrate have been disregarded since they have been shown to contribute by less than 15% to these potentials and have not a dominant influence on the adsorbate properties.^{17,18} The electrostatic interactions between the adsorbate and the periodic substrate are expanded in the 2D reciprocal space of the substrate, in order to achieve a fast convergence of the calculations.

The TIP4P model is used to describe the interaction V_{ww} between water molecules.¹⁹ The H₂O–HCl interaction V_{wp} is described on the basis of the model proposed by Kroes and Clary.⁴ Three charges are distributed on the H and Cl atoms, and on an additional site shifted along the HCl molecular axis, in order to represent the electrostatic interaction, and a 6-exponential expression is used to describe the dispersion-repulsion contribution. For the HCl–HCl potential V_{pp} , the electrostatic contribution comes from the interaction between point multipoles (up to the quadrupolar order) distributed on H, Cl, and on the center of the HCl bond.²⁰ An atom–atom Lennard-Jones potential²¹ represents the dispersion-repulsion interaction. For the set of V_{ww} , V_{wp} , and V_{pp} interactions, the sum is performed in the direct space, with a cutoff distance of 13.0 Å which gives almost the same results when using the Ewald summation procedure.²² Note that the models used here for water and HCl are not polarizable.

2. Details of the simulation

The main characteristics of our simulations have been already detailed in a previous paper devoted to the study of the dynamics of a water film adsorbed on MgO(001).¹⁵ They are briefly summarized here. To be consistent with the experimental coverages, the simulated water film contains 796 moving molecules forming five layers on a rigid MgO support. This film is about 18 Å thick along the *z* axis normal to the surface (*z*=0 is the MgO surface). The (*x*,*y*) sizes of the simulation box (*x*=35.9 Å and *y*=38.9 Å) along the directions parallel to the MgO surface obey the requirement of commensurability between the five water layers and the substrate geometry. This MD box corresponds to a repeated patch of size $12a_s \times 13a_s$, where $a_s = 2.99$ Å is the substrate unit cell parameter. At the beginning of the simulation, 156 water molecules are arranged in a flat monolayer directly above the substrate, whereas the remaining molecules form four upper bilayers having the hexagonal structure of pure ice. Each bilayer contains 160 water molecules.^{15,16}

The HCl coverage Θ_{HCl} is defined with respect to the number of Mg surface sites in the simulation box (i.e., 156 Mg sites). Three coverages are simulated in close similarity with the experiments (paper I), namely, 0.3, 0.6, and 1.0 ML. These three values correspond respectively to 47, 94, and 156 HCl molecules in the simulation box. Since the equilibrium distance between HCl molecules in the liquid phase is around 3.7 Å,²³ a coverage of 0.3 ML corresponds approximately to one complete layer of HCl molecules above the ice

film. Note that in experiments¹⁴ the HCl coverage unit (1 ML) is defined as 1 HCl molecule adsorbed per Mg surface site.

The translational equations of motion are solved using the Verlet algorithm, and a predictor-corrector method based on the quaternion representation of the molecular orientations is used for the orientational equations of motion, with a time step of 2.2 fs. The admolecules are treated as rigid bodies. Long time runs are performed, involving 250 000 time steps (i.e., 550 ps) of equilibration and 100 000 additional time steps (220 ps) of production for collecting the data. According to the experiments, simulations at eight different temperatures are carried out between 190 and 250 K.

3. Structure and dynamics of the adsorbate

The translational ordering of the admolecules is studied at each temperature through the analysis of the distribution function $p(z)$, where z defines the distance of the admolecule center of mass to the MgO surface plane. In the same way, the orientational ordering of the admolecules is characterized by the distribution functions of the Euler angles defining the orientations of the water and HCl molecules with respect to the absolute frame.

Moreover, in order to determine quantitatively the influence of the HCl adsorption on the water molecules ordering, we calculate translational (S_T) and orientational (S_R) order parameters that characterize the displacements of the water molecules from their ideal positions in ice Ih, when the temperature is increased.^{7,15,24} For the perfect proton ordered ice crystal, S_T and S_R are normalized to 1, while they vanish for the liquid.

The translational dynamics of the admolecules is determined¹⁵ through the calculation of self-diffusion coefficients from the linear behavior at long times of the mean square displacements of the molecular centers-of-mass.²⁵ In the same way, the orientational dynamics of the adsorbate is studied through the calculation of the time autocorrelation function $C_1(t)$ of the first Legendre polynomial P_1 . This function is plotted in the logarithmic form since the orientational diffusion coefficient is associated with the limiting linear behavior of $0.5 \ln C_1(t)$ at times much longer than the angular velocity correlation time.²⁶

B. Results

1. Structure of the adsorbed film

The distribution functions $p_{\text{HCl}}(z)$ for the HCl molecules and $p_w(z)$ for the H₂O molecules in the water film adsorbed on MgO are shown in Fig. 1 at various temperatures, and for a HCl coverage equal to 0.3 ML. The single peak evidenced at 2.12 Å in $p_w(z)$ at all temperatures corresponds to the signature of the flat water monolayer adsorbed directly on MgO. By contrast, the translational ordering of the upper water layers strongly depends on the temperature. At 190 K, $p_w(z)$ exhibits regularly distributed double peaks characterizing the successive water bilayers in the hexagonal ice structure. At the same temperature, $p_{\text{HCl}}(z)$ exhibits three main features around 11.5, 15.0, and 19.5 Å, indicating that the HCl molecules are located into three well-defined re-

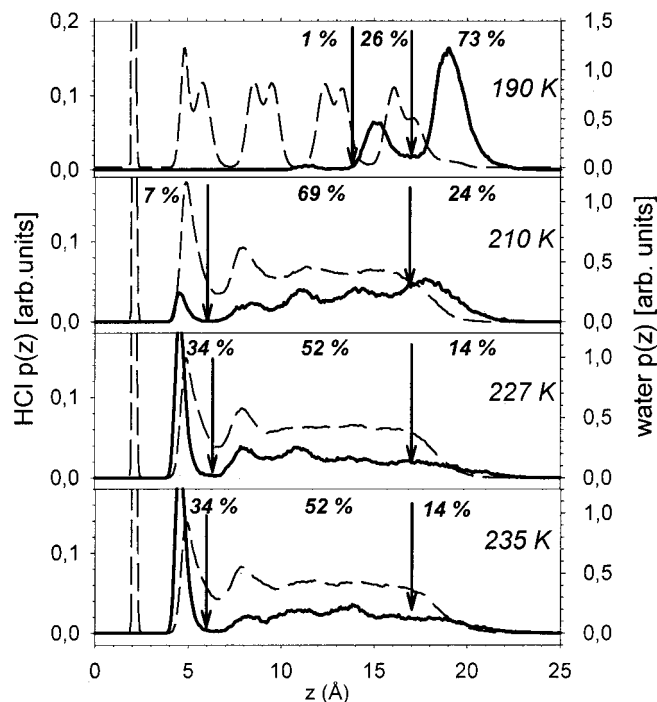


FIG. 1. Distribution functions (in arbitrary units) p_w and p_{HCl} of the distance z (Å) between the water (broken curve) or HCl (full curve) molecular centers of mass and the MgO surface (taken at $z=0$), at different temperatures. The HCl coverage is equal to 0.3 ML. Arrows indicate artificial boundaries corresponding to the ice/gas interface ($z \sim 17$ Å), outermost bilayer ($z \sim 13.5$ Å), innermost layer ($z \sim 6$ Å). Three regions are thus defined for $T \geq 210$ K, connected to surface sites, to core sites, and to MgO/ice interface sites for the HCl molecules. The percentage of deposited molecules that lie in each region is given.

gions. The number of HCl molecules in each region is given by the area of the corresponding peak in $p_{\text{HCl}}(z)$. These calculations indicate that most of the HCl molecules (73%) are located at the surface of the water film (peak p_L at 19.5 Å). Among the remaining molecules, 26% are incorporated preferentially between the first two outermost water bilayers at 15.0 Å, while 1% only are deeper in the film (at 11.5 Å).

Increasing slightly the temperature has a strong effect on the ordering of the H₂O and HCl molecules. At 210 K, the doublet structure of p_w disappears and it is replaced by more or less visible oscillations, indicating an increasing disorder of the water molecules. The distribution $p_{\text{HCl}}(z)$ is spread out into the whole water film, and 7% of the molecules are trapped near the flat water layer close to the MgO surface (small peak p_B at 4.5 Å), while only 24% of the HCl molecules still remain at the gas/film interface. Above 227 K, the population of the distribution peak close to the flat monolayer saturates (34% of the HCl molecules), and most of the HCl molecules lie inside the water film, with a nearly homogeneous distribution along the z coordinate.

For larger HCl coverages (0.6 and 1.0 ML), the distribution functions $p_w(z)$ and $p_{\text{HCl}}(z)$ are given in Figs. 2 and 3 as functions of temperature. The z translational ordering of the water film appears to be nearly independent of the HCl coverage, since $p_w(z)$ exhibits the monolayer + hexagonal bilayer structure at 190 K and a disorder that increases up to the liquid-like behavior above 235 K, as already obtained

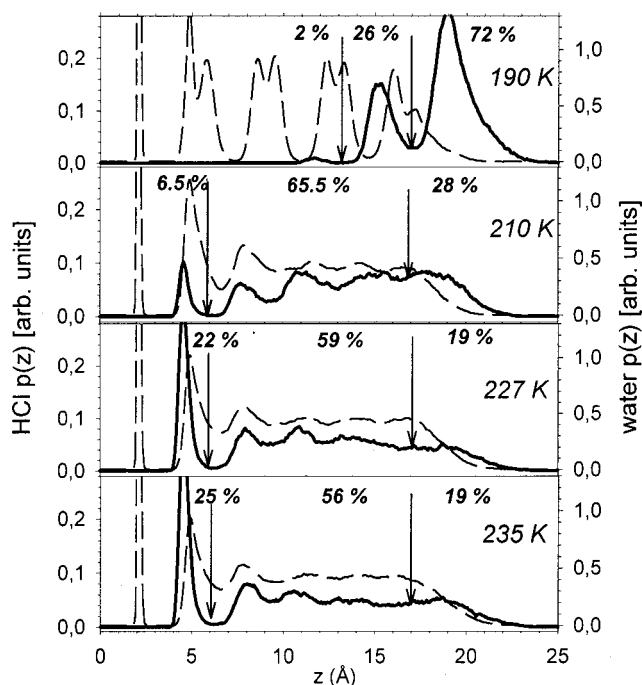


FIG. 2. Same as Fig. 1 for a HCl coverage equal to 0.6 ML.

with the lower HCl coverage. The distribution functions $p_{\text{HCl}}(z)$ for the larger coverages have also a similar behavior. At 190 K and $\Theta_{\text{HCl}}=0.6$ ML, the HCl molecules are mainly located at the surface of the water film, since only 26% cross over the surface water bilayer, and no more than 2% penetrate deeper into the water film. When the HCl coverage increases to 1.0 ML, a doublet occurs in $p_{\text{HCl}}(z)$ at the ice surface, around 18.5 and 21.5 Å which indicates that the HCl molecules form two layers above the water film. The per-

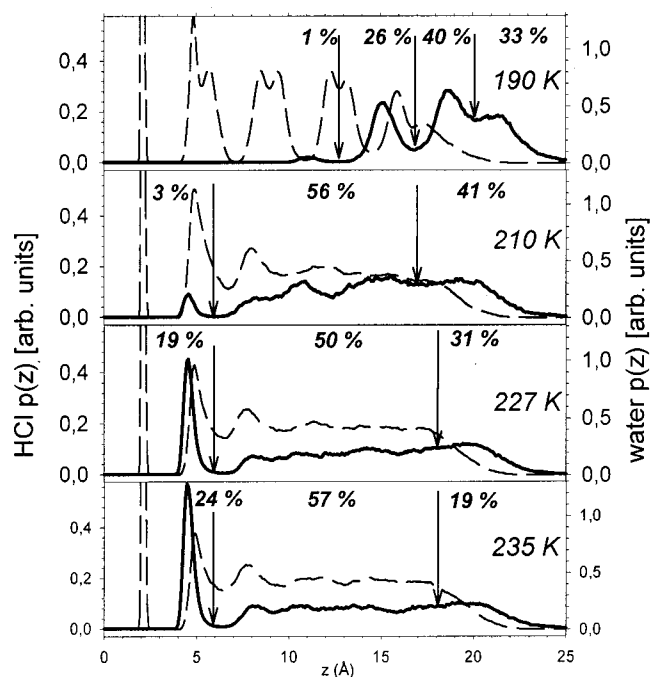


FIG. 3. Same as Fig. 1 for a HCl coverage equal to 1.0 ML.

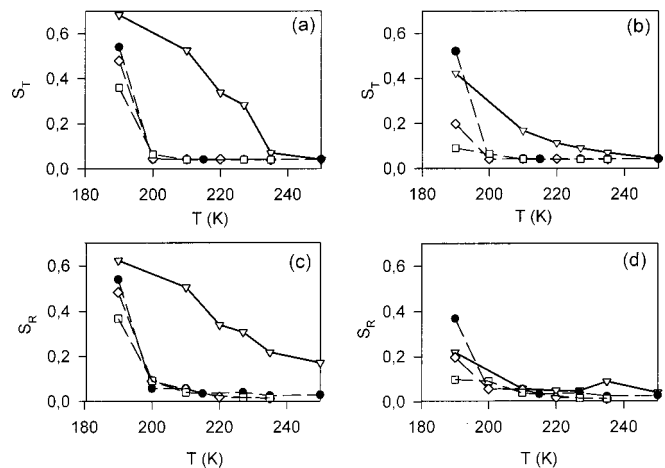


FIG. 4. Translational order parameter S_T vs temperature for (a) the whole ice film and (b) the outermost layer, only. Orientational order parameter S_R vs temperature for (c) the whole ice film and (d) the outermost layer, only. The different symbols correspond to different HCl coverage: 0 ML (∇), 0.3 ML (\bullet), 0.6 ML (\diamond), and 1.0 ML (\square).

centage of HCl molecules corresponding to this doublet is still 73%, with a nearly equal percentage assigned to each peak in the doublet.

At higher temperature, the HCl molecules diffuse throughout the water film and the same percentage reaches the flat monolayer at $\Theta_{\text{HCl}}=0.6$ and 1.0 ML. At 235 K, and for both coverages, around 55% of the HCl molecules are distributed in the bulk ice film, while 19% remains at the gas/ice interface. The intensity of the single peak of $p_{\text{HCl}}(z)$ close to the MgO substrate, at around 4.5 Å, corresponds to 25% of the HCl molecules. For these HCl coverages, it appears that this distribution peak cannot be saturated in the temperature range of the present study, since its population continuously increases with temperature up to 250 K (not shown).

The translational S_T and orientational S_R order parameters for the whole water film (except the monolayer) and its outermost layer are given in Fig. 4 as functions of temperature and HCl coverage. At 190 K, the water translational ordering decreases from 0.7 for the pure ice film to 0.4 when the HCl coverage increases from 0.3 to 1.0 ML, as shown in Fig. 4(a). The disorder increases regularly with T and becomes complete at 230 K for the pure ice film. This disordering appears at 200 K when HCl is present. The same behavior is observed for the outermost layer [Fig. 4(b)], which exhibits however much more disorder than the water film, even at 190 K. Similar conclusions can be drawn from the analysis of S_R [Figs. 4(c) and 4(d)] which shows that rotational order totally disappears above 200 K, for the outermost water layer as well as for the whole film.

Note that a singular behavior is obtained for $\Theta_{\text{HCl}}=0.3$ ML [Figs. 4(b) and 4(d)]. Indeed, at 190 K, the outermost water layer appears more structured than the pure ice film surface. This feature can be interpreted as the result of a competition between the HCl ordering influence at the ice surface and the HCl disordering in bulk ice. Indeed, such a HCl coverage corresponds approximately to the formation of a monolayer which acts as a “ceiling” above the water film,

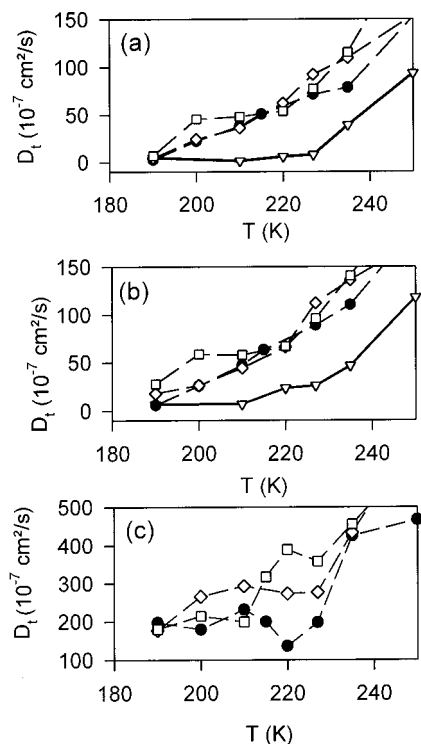


FIG. 5. Translational diffusion coefficient D_t ($10^{-7} \times \text{cm}^2 \text{s}^{-1}$) vs temperature as a function of HCl coverage; (a) for the whole water film, (b) for the outermost water layer, and (c) for the HCl molecules. The different symbols correspond to different HCl coverage: 0 ML (∇), 0.3 ML (\bullet), 0.6 ML (\diamond), and 1.0 ML (\square).

and tends to order the H_2O molecules of the surface by forming additional H-bonds. As a consequence, the outermost water layer that is in contact with the HCl layer is more ordered than the same outermost layer of the free surface with dangling bonds. At higher HCl coverages, the strengthening of the outermost water layer by the HCl ceiling is nearly the same due to H-bond saturation, but the molar fraction of HCl: H_2O inside the ice interface increases significantly. This HCl penetration into bulk ice disrupts the hydrogen bond network of the outermost water layer, leading to a disorder increase in the bulk. This latter effect predominates in the competition with the HCl surface ordering, which results in a decrease of the order parameters of doped ice when compared to pure ice.

2. Dynamics of the admolecules

Figures 5(a) and 5(b) show the calculated translational diffusion coefficients D_t for the water molecules of the supported ice film as a function of temperature and HCl coverage. It is clearly demonstrated that the translational mobility of the water molecules is strongly enhanced by the presence of HCl, for all the temperatures higher than 190 K, in the bulk as at the surface of the film. For instance, at 220 K, D_t increases by a factor of 6 when Θ_{HCl} increases from 0 to 1.0 ML. The curves of translational mobility for the water molecules behave similarly with the HCl coverage. A more or less monotonic increase of the diffusion coefficient is observed for all the coverages.

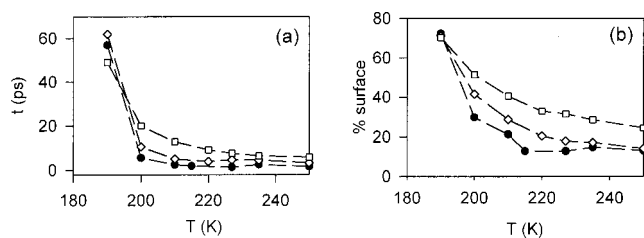


FIG. 6. (a) Mean residence time (ps) and (b) mean proportion of HCl molecules at the ice surface vs temperature, for the three HCl coverages: 0.3 ML (\bullet), 0.6 ML (\diamond), and 1.0 ML (\square).

The translational diffusion coefficients for the HCl molecules, only, are shown in Fig. 5(c), as a function of temperature and HCl coverage. Whatever the temperature, the HCl molecules are much more mobile than water, since the corresponding values of the translational diffusion coefficients are one order of magnitude greater for HCl than for H_2O . The shape of D_t for HCl strongly depends on the coverage, especially between 210 and 240 K, where three different behaviors are evidenced. Indeed, for $\Theta_{\text{HCl}} = 0.3$ ML, the HCl mobility is minimum around 220 K, and then increases significantly. This behavior can be correlated to the distribution function $p(z)$ shown in Fig. 1. Indeed, below 210 K, the HCl molecules are mainly localized above the water film, where they are characterized by their own mobility. Above 210 K, they penetrate into the water film, and reach the ice–MgO interface where their dynamics is hindered by the interaction with the water molecules of the flat monolayer. The saturation of the distribution peak p_B is obtained around 220–230 K, and this temperature corresponds to the minimum in the HCl mobility curve [Fig. 5(c)]. Above 220 K, both the translational mobility of the surrounding water molecules, and the own dynamics of the HCl molecules tend to counterbalance the trapping effect at the solid interface, leading to an increase of the HCl mobility. For larger HCl coverages (0.6 and 1.0 ML), the saturation of the peak p_B near the ice–MgO interface cannot be achieved and, above 210 K, a large amount of HCl molecules are spread out into the whole water film. Since most of the HCl molecules are not trapped at the solid interface, their mobility is high due to the rapid dynamics of the water molecules in the film. As a consequence, no minimum is observed in the corresponding D_t curves.

3. Residence times of HCl at the ice surface

In order to characterize the dynamics of the HCl molecules, we have also calculated their residence times at the gas/water interface (i.e., for $z \geq 17$ Å), as functions of temperature and HCl coverage. The residence time of HCl is defined as the mean time spent by these admolecules in the adsorption site characterized by the peak p_L in $p_{\text{HCl}}(z)$. Note that the number of HCl molecules that are expelled from the surface site towards the gas phase has been found to be vanishingly small ($\leq 1\%$) even at 250 K, within the simulation duration. Therefore, the residence time mainly refers to loss of HCl from the surface to the bulk and not to the gas phase.

Figure 6(a) shows that the average lifetime of HCl at the surface of ice is nearly coverage independent, when this cov-

erage does not exceed 0.6 ML. It strongly decreases with the temperature, from about 60 ps at 190 K to a constant value equal to 10 ps above 210 K. At higher coverage ($\Theta_{\text{HCl}} = 1.0$ ML), the lifetime behavior exhibits a similar shape, but the decrease is much less abrupt, from 50 ps at 190 K to 20 ps at 200 K. These features can be correlated to the evolution with temperature and coverage of the hydracid population in the trapping site at the ice film surface [Fig. 6(b)]. Such a population is defined as the average proportion of HCl molecules that stay at the surface sites during the whole simulation time, including the molecules that leave these sites and come back into them during the simulation. At 190 K, 70% of the HCl molecules lie at the surface site for the three coverages considered, whereas this population decreases with temperature down to about 15% at 250 K for the two lowest coverages, and to about 25% for $\Theta_{\text{HCl}} = 1$. These two proportions correspond to equilibrium situations for which the number of HCl molecules at the surface site become approximately constant. It may be outlined that this number varies significantly since it depends on the initial HCl dose deposited on the surface. Note that counting the HCl molecules gives approximately the same results as estimating the integrated area of the peaks in the distribution function $P_{\text{HCl}}(z)$.

III. DISCUSSION

In the present classical MD simulations, new information is provided on the dynamic behavior of an ultrathin ice film doped by HCl molecules. This information can be compared to previous calculations¹⁵ carried out according to the same approach for the same film of pure ice. When $T \leq 190$ K, the quasi-hexagonal ice traps the HCl molecules at its free surface, or in a less extent, at the outermost bilayer sites, whatever the HCl coverage. At higher temperature ($T \geq 200$ K), the film structure appears more and more disordered, as shown by the behavior of the translational and orientational order parameters (Fig. 4). The temperature range of $T = 190$ – 200 K thus corresponds to an order–disorder transition for the ice film structure at any coverage ($\Theta_{\text{HCl}} \leq 1.0$ ML), with a sudden decrease of the order parameters S_T and S_R . For comparison, these parameters for the pure ice film tend to vanish with a much smoother slope around 230 K, i.e., at a temperature that is significantly higher.^{15,24} This disorder can be assigned to the formation/breaking of H-bonds between HCl and H₂O molecules, instead of the most regular H-bond structuration between water molecules. Note that this feature, which indicates the influence of the HCl molecule on the ice structure and dynamics, has been already underlined by Gertner and Hynes.⁷ In addition, these authors also discussed the influence of the HCl ionization on the ordering/disordering process of the ice surface, assuming however an infinite HCl dilution.

The diffusion coefficient of H₂O molecules in the HCl-doped ice film obeys the same law versus the temperature. While its value is the same for the doped and pure films at 190 K, a temperature raise strongly enhances the water diffusion in the HCl-doped film. This indicates the highly dynamic nature of the H₂O motions in presence of HCl, when compared to a pure ice film.

Considering now the HCl behavior on/in the ice film, the striking result shown by Figs. 1–3 is the different behavior of the HCl kinetics in the film below and above 200 K. At 190 K, as already mentioned, the HCl molecules remain trapped at the ice interface, while at 210 K, the HCl diffusion inside the film is very easy. A further increase of T up to 235 K does not change fundamentally the distribution shape of HCl in the film. The equilibrium distribution is nearly reached around 230 K, with about 55% of HCl molecules inside the core of the film, while the remaining percentage is shared between the two interfaces. The relative proportion of molecules at the MgO/ice interface is generally larger than at the ice/gas interface, whatever the initial HCl coverage for $\Theta_{\text{HCl}} \leq 1.0$ ML.

The collective influence of the HCl molecules can be quantified by comparing the mean residence time of HCl in the surface site, when a single HCl is present, with the mean times obtained in the present paper by increasing the HCl dose up to 1.0 ML [Fig. 6(a)]. At 200 K, the mean residence time for the single HCl molecule is around 90 ps.¹³ It decreases by one order of magnitude when the coverage increases up to 0.6 ML, and by a factor 4.5 at one monolayer coverage. This feature can be interpreted as the increasing influence of the HCl/H₂O dynamics when the HCl dose increases, while the strengthening of the mutual interactions between HCl molecules at 1.0 ML tends to limit the effect of this dynamics. At much higher temperature ($T = 250$ K), the values of the residence time vary from 2 to 6 ps according to the coverage and they are smaller than the value calculated for the single molecule (around 20 ps).²⁷

Before comparing the present results with the experimental data, the limits of the classical molecular dynamics simulations must be clearly defined. In contrast with *ab initio* approaches,²⁸ the present technique is unable to account for the chemical processes that are generally invoked regarding the inclusion of HCl in water or ice. Especially, the ionization of HCl and dissociation at the surface, interface or core of the ice film cannot be taken into account. Diffusion in the present model refers to the molecular species, and chemical mechanisms that can dramatically influence this diffusion is disregarded. For the same reason, it is also impossible, within this model, to understand the formation of hydrates at the surface or into the bulk film.^{14,29,30} In addition, the potentials used to describe H₂O–H₂O, H₂O–HCl, and HCl–HCl interactions are semiempirical, and the accuracy of the simulation calculations rests on the accuracy of these potentials. The TIP4P potential is generally considered as being among the most simple and adequate form to account for the ice properties, which can be used in simulations.²⁴ However, it is known to have some drawbacks, regarding especially the underestimate of the surface melting temperature by around 25–30 K.³¹ Refined versions of this potential, including the polarization of the water molecules are available, which improve the comparison with some experimental data on ice, but still fail to interpret other ice properties.³² Since the simplest version of the TIP4P potential is used here, the present results should be regarded from a qualitative point of view, i.e., by comparing the HCl doped film properties relatively to the pure film.

Within the limits of the present approach, the comparison of the experimental data obtained in paper I,¹⁴ and the results of simulations carried out in the same conditions provides some information on the molecular behavior of the system "HCl-doped ice film." At 190 K, the fact that the neutron scattering spectra indicates no appreciable disturbance of the ice structure due to HCl adsorption can be interpreted as the result of the trapping of most of the HCl molecules at the ice surface. Even for $\Theta_{\text{HCl}}=1.0$ ML, the HCl molecules do not form an ordered phase, and the neutrons probe the ordered structure of the ice film, only. When $T \geq 210$ K, the partial destruction of the Ih structure of ice observed in experiments can be explained by the easy diffusion of HCl into the film, which leads to a large disordering of the ice structure. The fact that some order still persists in the film is assigned to the influence of the MgO support which, through the existence of the flat water monolayer, tends to keep an order in the innermost layers. Note, however, that the HCl ionization could also participate to the order loss in the film.⁷ Moreover, the calculations are able to interpret the mobility increase of ice with the coverage when Θ_{HCl} remains smaller than 0.6 ML, and the occurrence of a liquid phase around 250 K which accounts for about 30%–45% of the ice film thickness. Indeed, the profiles of ice density, the shapes of the order parameters S_T and S_R , and the values of the diffusion coefficients as functions of T and Θ_{HCl} are sufficiently consistent to interpret the ice behavior above 230 K in terms of the occurrence of a liquidlike phase. The MD simulations can explain qualitatively the lowering of the melting temperature by about 15–20 K when the ice film is doped by HCl. A quantitative agreement would require to shift the calculated temperatures for the doped and pure ice films by about 30 K, as explained before.¹⁵ Furthermore, at higher temperatures, our calculations cannot reproduce the strong decrease of the molecule mobility assigned in the experiments to the hydrate formation, due to the limits of the model as already mentioned.

The present results can be compared to available data issued from combined isothermal desorption depth profiling and laser induced thermal desorption probing,^{33,34} and from combined infrared reflection absorption spectroscopy and temperature programmed desorption.^{29,35} Starting from the analysis of their experiments of desorption and diffusion kinetics, carried out on HDO diffusion in ultrathin HNO_3 - and HCl-doped crystalline D_2O ice multilayers in a temperature range 140–175 K, George and co-workers^{33,34} extrapolated their results at stratospheric temperatures. They predicted that the presence of HNO_3 and HCl considerably increased and decreased the H_2O surface residence times when compared to the pure ice film, respectively. More generally, they concluded that the acid molecules should alter dramatically the growth, stability, and lifetimes of atmospheric ice particles. Observation of adsorbed and absorbed states for HCl on ice between 140 and 180 K was made by Graham and Roberts,^{29,35} who concluded to the presence of two sites for HCl, one site corresponding to molecularly adsorbed HCl and the other site associated with dissociated HCl in bulk ice. They also inferred³⁵ the formation of amorphous hexahydrate crystallized at 165 K for a convenient HCl/ H_2O stoichi-

ometry, and the existence of pure ice and pure $\text{HCl}:\text{6H}_2\text{O}$ species when the HCl: H_2O ratio was less than 1:6. Although these experiments were conducted at too low temperatures to be easily transferable to stratospheric ice, they qualitatively corroborate the strong influence of HCl on the water mobility shown in simulations.

IV. CONCLUSION

For the first time, experiments and simulation calculations have been performed together on the same system, i.e., a 5 BL thick ice film doped by adsorption of HCl molecules up to 1.0 ML, at the stratospheric temperatures ranging from 190 to 270 K. Within this context, it has been shown that a molecular interpretation of the H_2O and HCl dynamics can be reached, especially by explaining the temperature lowering of the doped ice melting when compared to pure ice. This study is probably too ideal when compared to the intricate mechanisms that can be invoked in polar stratospheric clouds. It especially disregards the generally admitted situation concerning the hydracid ionization at the ice surface, which can only be taken into account in much more time consuming approaches. Such approaches, based on quantum mechanical calculations, are however limited to infinite dilution of HCl, a situation which is far from the present experimental conditions.

- ¹S. Solomon, *Rev. Geophys.* **26**, 131 (1988).
- ²M. J. Molina, *Chemistry of the Atmosphere: Its Impact on Global Change* (Blackwell Scientific, Oxford, 1994).
- ³D. R. Hanson and A. R. Ravishankara, *J. Phys. Chem.* **96**, 268 (1992).
- ⁴G. J. Kroes and D. C. Clary, *J. Phys. Chem.* **96**, 7079 (1992); *Geophys. Res. Lett.* **19**, 1355 (1992).
- ⁵B. J. Gertner and J. T. Hynes, *Science* **271**, 1563 (1996).
- ⁶L. Wang and D. C. Clary, *J. Chem. Phys.* **104**, 5663 (1996).
- ⁷B. J. Gertner and J. T. Hynes, *Faraday Discuss.* **110**, 301 (1998).
- ⁸M. Svanberg, J. B. C. Pettersson, and K. Bolton, *J. Phys. Chem. A* **104**, 5787 (2000).
- ⁹S. Re, Y. Osamura, Y. Suzuki, and H. F. Shaeffer III, *J. Chem. Phys.* **109**, 973 (1998).
- ¹⁰A. Allouche, I. Couturier-Tamburelli, and T. Chiavassa, *J. Phys. Chem. B* **104**, 1497 (2000).
- ¹¹G. J. Kroes, *Comments At. Mol. Phys.* **34**, 259 (1999).
- ¹²C. Girardet and C. Toubin, *Surf. Sci. Rep.* **44**, 159 (2001).
- ¹³C. Toubin, P. N. M. Hoang, S. Picaud, and C. Girardet, *Chem. Phys. Lett.* **329**, 331 (2000).
- ¹⁴B. Demirdjian, D. Ferry, J. Suzanne, C. Toubin, S. Picaud, P. N. M. Hoang, and C. Girardet, *J. Chem. Phys.* **116**, 5143 (2002), preceding paper.
- ¹⁵C. Toubin, S. Picaud, P. N. M. Hoang, C. Girardet, B. Demirdjian, D. Ferry, and J. Suzanne, *J. Chem. Phys.* **114**, 6371 (2001).
- ¹⁶A. Marmier, P. N. M. Hoang, S. Picaud, C. Girardet, and R. M. Lynden-Bell, *J. Chem. Phys.* **109**, 3245 (1998).
- ¹⁷C. Toubin, S. Picaud, and C. Girardet, *Chem. Phys.* **244**, 227 (1999).
- ¹⁸D. Ferry, S. Picaud, P. N. M. Hoang, C. Girardet, L. Giordano, B. Demirdjian, and J. Suzanne, *Surf. Sci.* **409**, 101 (1998).
- ¹⁹W. L. Jorgensen, J. Chandrasekhar, J. F. Madura, R. W. Impey, and M. L. Klein, *J. Chem. Phys.* **79**, 926 (1983).
- ²⁰A. J. Stone and M. Alderton, *Mol. Phys.* **56**, 1047 (1985).
- ²¹S. Murad, K. E. Gubbins, and J. G. Powles, *Mol. Phys.* **40**, 253 (1980).
- ²²R. S. Taylor, L. X. Dang, and B. C. Garret, *J. Phys. Chem.* **100**, 11720 (1996).
- ²³C. Votava, R. Ahlrichs, and A. Geiger, *J. Chem. Phys.* **78**, 6841 (1983).
- ²⁴G. J. Kroes, *Surf. Sci.* **275**, 365 (1992).
- ²⁵R. W. Impey, P. A. Madden, and I. R. McDonald, *Mol. Phys.* **46**, 513 (1982).

- ²⁶R. M. Lynden-Bell and I. R. McDonald, *Mol. Phys.* **43**, 1429 (1981).
- ²⁷C. Toubin, P. N. M. Hoang, S. Picaud, and C. Girardet, *J. Chem. Phys.* **113**, 1184 (2000).
- ²⁸K. Ando and J. T. Hynes, *J. Phys. Chem. B* **101**, 10464 (1997).
- ²⁹J. D. Graham and J. T. Roberts, *J. Phys. Chem.* **98**, 5974 (1994).
- ³⁰K. L. Foster, M. A. Tolbert, and S. M. George, *J. Phys. Chem. A* **101**, 4979 (1997).
- ³¹Y. A. Mantz, F. M. Geiger, L. T. Molina, M. J. Molina, and B. T. Trout, *J. Chem. Phys.* **113**, 10733 (2000).
- ³²S. W. Rick, *J. Chem. Phys.* **114**, 2276 (2001).
- ³³F. E. Livingston and S. M. George, *J. Phys. Chem. A* **102**, 10280 (1998).
- ³⁴F. E. Livingston and S. M. George, *J. Phys. Chem. B* **103**, 4366 (1999).
- ³⁵J. D. Graham and J. T. Roberts, *Chemom. Intell. Lab. Syst.* **37**, 139 (1997).